Energy Fuels **2010,** *24,* 1521–1528 · DOI:10.1021/ef9011005
Published on Web 02/09/2010

energy&fuels
article

Oxidation of C1−C5 Alkane Quinternary Natural Gas Mixtures at High Pressures

D. Healy,[†] D. M. Kalitan,[‡] C. J. Aul,[§] E. L. Petersen,[§] G. Bourque,[∥] and H. J. Curran*[,†]

[†]*Combustion Chemistry Centre, National University of Ireland, Galway, Ireland,* [‡]*Mechanical, Materials and Aerospace Engineering, University of Central Florida, Orlando, Florida 32816,* [§]*Department of Mechanical Engineering, Texas A&M University, College Station, Texas 77843, and* [∥]*Rolls-Royce Canada, Montreal, Canada*

Received September 29, 2009. Revised Manuscript Received January 19, 2010

Rapid compression machine (RCM) and shock-tube facilities have been employed to study the oxidation of natural gas blends at high pressure and intermediate to high temperatures. The use of both types of facilities allows a broad temperature envelope to be investigated and therefore encompasses the complete range applicable to gas turbines. A detailed chemical kinetic mechanism has been developed to simulate these results and will be used to approximate similar fuels. Mixtures of $CH_4/C_2H_6/C_3H_8/n\text{-}C_4H_{10}/n\text{-}C_5H_{12}$ have been studied in the temperature range 630−1550 K, in the pressure range 8−30 bar, and at equivalence ratios of 0.5, 1.0, and 2.0 in "air". For shock-tube experiments, the diluent gas was nitrogen, whereas in the RCM experiments the diluent gas composition ranged from pure nitrogen (at lower temperatures) to pure argon (at the highest temperatures). In addition, the combustion chamber in the RCM was fitted with a thermostat and heating tape to control and vary the initial temperature thereby varying the compressed gas temperature. Because the time-scale of a rapid compression machine experiment is so long, heat losses are significant. Thus, a series of nonreactive experiments were performed in order to account for the heat loss associated with each mixture composition and pressure.

1. Introduction

Natural gas blends are of particular importance to the gas turbine industry as they offer a more realistic parallel to the real composition of natural gas than their single-component counterparts. Fundamental measurements of the ignition delay time of blends of methane seeded with higher-order hydrocarbons at pressures and concentrations of interest to gas turbines are important for their design and efficient operation. While there is a significant quantity of data in the literature on single-component studies of methane, ethane, propane, butane, and/or pentane, until recently the study of multicomponent blends was not common. Numerous ignition delay studies of methane at high-temperatures and low-pressures have been carried out, reported, and summarized by Spadaccini and Colket.[1] Higher-pressure studies have also been carried out by Tsuboi and Wagner[2] and Petersen et al.[3] and more recently by Zhukov et al.[4] and Huang et al.[5]

Ignition delay studies of ethane, although present in the literature, are sparse, comprised of shock-tube studies between 1 and 8 bar and 1100 and 2000 K.[6−8]

Most ignition delay data for propane come from high-temperature shock-tube studies.[10−14] Although these studies cover a wide pressure range (0.75−500 bar) at both lean and rich conditions, the lowest temperature available in shock-tube studies was in the region of 900 K. Cadman et al.[15] reduced this temperature to 800 K by tailoring the driver gas, and these efforts were later expanded to higher pressures in the study of Zhukov et al.[16] Recently, Gallagher et al.[17] studied ignition delays of propane under rapid compression at lean to rich conditions and pressures of 21−37 bar. In their study, the temperature envelope was extended to 680 K.

n-Butane is another well-categorized hydrocarbon fuel with ignition delays having been studied in a number of regimes. Yoshizawa and Kawada[18] and Ogura et al.[19] studied ignition delays of *n*-butane at lean conditions behind reflected shock waves at 0.26−0.8 bar and 1.9−2.4 bar, respectively, in the temperature range 1000−1800 Koichi Hayashi and Goto[20] also studied ignition behind reflected shock waves and extended the temperature range downward to 780 K by tailoring

*To whom correspondence should be addressed. Telephone: 00353-91-493856. E-mail: henry.curran@nuigalway.ie.

(1) Spadaccini, L. J.; Colket, M. B., III. *Prog. Energy Combust. Sci.* **1994**, *20*, 431.
(2) Tsuboi, T.; Wagner, H. Gg. *Proc. Combust. Inst.* **1974**, *15*, 883.
(3) Petersen, E. L.; Davidson, D. F.; Hanson, R. K. *Combust. Flame* **1999**, *117*, 272.
(4) Zhukov, V. P.; Sechenov, V. A.; Starikovskii, A. Y. *Combust., Explosions, Shock Waves* **2003**, *30*, 487.
(5) Huang, J.; Hill, P. G.; Bushe, W. K.; Munshi, S. R. *Combust. Flame* **2004**, *136*, 25.
(6) Burcat, A.; Crossley, R. W.; Scheller, K.; Skinner, G. B. *Combust. Flame* **1972**, *18*, 115.
(7) Cooke, D. F.; Williams, A. *Combust. Flame* **1975**, *24*, 245.
(8) de Vries, J.; Hall, J. M.; Simmons, S. M.; Rickard, M. J. A.; Kalitan, D. M.; Petersen, E. L. *Combust. Flame* **2007**, *150*, 137.
(9) Higgin, R. M. R.; Williams, A. *Proc. Combust. Inst.* **1969**, *12*, 579.
(10) Kim, K.; Shin, K. S. *Bull. Korean Chem. Soc.* **2001**, *22*, 303.
(11) Horning, D. C.; Davidson, D. F.; Hanson, R. K. *J. Prop. Power* **2002**, *18* (2), 363.
(12) Herzler, J.; Jerig, L.; Roth, P. *Combust. Sci. Technol.* **2004**, *176* (10), 1627.
(13) Penyakov, O. G.; Ragotner, K. A.; Dean, A. J.; Varatharajan, B. *Proc. Combust. Inst.* **2005**, *30*, 1941.
(14) Dagaut, P.; Cathonnet, M.; Boettner, J. C. *Int. J. Chem. Kinet.* **1992**, *24*, 813.
(15) Cadman, P.; Thomas, G.; Butler, P. *Phys. Chem. Chem. Phys.* **2000**, *2*, 5411.
(16) Zhukov, V. P.; Sechenov, V. A.; Starikovskii, A.Yu. *Kinet. Katal.* **2005**, *46*, 319.
(17) Gallagher, S.; Curran, H. J.; Metcalfe, W. K.; Healy, D.; Simmie, J. M.; Bourque, G. *Combust. Flame* **2008**, *153*, 316.
(18) Yoshizawa, Y.; Kawada, H. *Bull. JSME* **1971**, *16*, 576.
(19) Ogura, T.; Nagumo, Y.; Miyoshi, A.; Koshi, M. *Energy Fuels* **2007**, *21*, 130.
(20) Koichi Hayashi, A.; Goto, M. *AIP Conf. Proc.* **1990**, *208*, 713.

Table 1. Composition (% Volume) of Natural Gas[9]

component	Russian	Abu Dhabi	Indonesia	Algerian
CH_4	96.24	82.07	89.91	89.533
C_2H_6	1.17	15.86	5.44	8.367
C_3H_8	0.34	1.89	3.16	1.197
i-C_4H_{10}	0.05	0.07	0.67	0.166
n-C_4H_{10}	0.08	0.06	0.75	0.226
i-C_5H_{12}	0.02		0.03	0.016
C_6+	0.04			
N_2	1.79	0.05	0.04	0.495
CO_2	0.26			

the driver gas and seeding the fuel with traces of carbon dioxide. Horning et al.[11] extended the scope of *n*-butane ignition delay records in this temperature range while studying ignition of *n*-alkanes behind reflected shocks reporting ignition at 1−6 bar and equivalence ratios of 0.5−2.0. Low-temperature ignition delays for *n*-butane, mostly from rapid compression machine studies, also exist with the data covering pressures of 10 − 20 bar from fuel lean to stoichiometric conditions.[21−24]

Ignition delay times for *n*-pentane have been measured under rapid compression[25,26] and behind reflected shocks in the recent work reported by Zhukov et al.[27] With such a wealth of data on each particular hydrocarbon, it is logical that the next stepping stone in this research would be to investigate blends of these components, as natural gas itself is known to be a multicomponent mixture of hydrocarbons which also contains small amounts of N_2, CO_2, O_2, H_2 as well as some particulates. Typical compositions of natural gas are provided in Table 1.

Most ignition delay time measurements of hydrocarbon blends are sourced from shock-tube studies with only a handful of studies carried out in a rapid compression machine. Table 2 gives a condensed overview of the range of studies that are currently available which are dedicated to this field of study. Recently, Heyne et al.[28] measured ignition delay times in a rapid compression machine (RCM) at the University of Lille for $CH_4/C_2H_6/C_3H_8$ mixtures representative of an average natural gas composition. The pressure at the end of compression (EOC) varied from 13 to 21 bar, and the core gas temperature ranged from 850 to 925 K. Zero-dimensional modeling starting from the EOC was used to reproduce the experimental ignition delay times taking into account heat losses during the preignition phase. The experimental database served as a basis for the development of a reaction mechanism suitable for HCCI like autoignition simulations on a stationary cogeneration engine with a prechamber. Different mechanisms for natural gas oxidation and combustion were tested and their low temperature simulation ability investigated, showing difficulties to properly reproduce the low-temperature ignition delay times. A detailed chemical kinetic mechanism was used to simulate these data, starting from the GRI3.0 mechanism with the addition of a submodule improving the low-temperature chemistry representation. The resulting optimized mechanism was also tested on experimental shock-tube data between 900 and 1250 K and gave satisfying results within the temperature range where the optimization was performed.

Gersen et al.[29] investigated changes in the autoignition behavior of methane, the primary component of natural gas, upon hydrogen addition in a rapid compression machine (RCM). Ignition delay times were measured under stoichiometric conditions at pressures between 15 and 70 bar and temperatures between 950 and 1060 K; the hydrogen fraction in the fuel varied between 0 and 1. Ignition delay times in methane/hydrogen mixtures were well correlated with the ignition delay times of the pure fuels by using a simple mixing relation reported by Cheng and Oppenheim.[30] Simulations of the ignition delay times using various chemical mechanisms were also reported. The mechanism given by Petersen et al.[31] showed excellent agreement with the measurements for all mixtures studied. Initial results on fuel-lean mixtures show a modest effect of equivalence ratio on the delay times.

Healy et al.[32] studied the oxidation of methane/propane mixtures in "air" for blends containing 90% CH_4/10% C_3H_8 and 70% CH_4/30% C_3H_8 over the temperature range 740−1550 K, at compressed gas pressures of 10, 20, and 30 bar, and at varying equivalence ratios of 0.3, 0.5, 1.0, 2.0, and 3.0 in both a high-pressure shock tube and in a rapid compression machine. These data are consistent with other experiments presented in the literature for other alkane fuels in that, when ignition delay times are plotted as a function of temperature, a characteristic negative coefficient behavior was observed, particularly for mixtures containing 30% propane. These data were simulated using a detailed chemical kinetic model with overall good agreement with the experiment.

Subsequently, Healy et al.[33] studied the oxidation of methane/ethane/propane mixtures, for blends containing 90/6.6/3.3, 70/15/15, and 70/20/10% by volume of each fuel, respectively, in "air", over the temperature range 770−1580 K, at compressed gas pressures of approximately 1, 10, 20, 30, 40, and 50 bar, and at equivalence ratios of 0.5, 1.0, and 2.0. This work represented the most comprehensive set of methane/ethane/propane ignition delay time measurements available in a single study which extended the composition envelope over an industrially relevant pressure range. It was also the first such study to present ignition delay times at significantly overlapping conditions from both a rapid compression machine and a shock tube.These data were also simulated with a detailed chemical kinetic model with overall good agreement observed.

Most recently, we have reported on the oxidation of $CH_4/C_2H_6/C_3H_8/n$-C_4H_{10}/n-C_5H_{12}[34] in our laboratories. Ignition delay times were measured in two different shock tubes and in a rapid compression machine at pressures up to 34 bar and

(21) Carlier, M.; Corre, C.; Minetti, R.; Pauwels, J.-F.; Ribaucour, M.; Sochet, L. R. *Proc. Combust. Inst.* **1990**, *23*, 1753.
(22) Griffiths, J. F.; Halford-Maw, P. A.; Rose, D. J. *Combust. Flame* **1993**, *95*, 291.
(23) Minetti, R.; Ribaucour, M.; Carlier, M.; Fittschen, C.; Sochet, L. R. *Combust. Flame* **1994**, *96*, 201.
(24) Kim, H.; Lim, Y.; Min, K.; Lee, D. *KSME Int. J.* **2002**, *16* (8), 1127.
(25) Westbrook, C. K.; Curran, H. J.; Pitz, W. J.; Griffiths, J. F.; Mohamed, C.; Wo, S. K. *Proc. Combust. Inst.* **1998**, *27*, 371.
(26) Minetti, R.; Roubaud, A.; Therssen, E.; Ribaucour, M.; Sochet, L.-R. *Combust. Flame* **1999**, *118*, 213.
(27) Zhukov, V. P.; Sechenov, V. A.; Starikovskii, A. Yu. *Combust. Flame* **2005**, *140*, 196.
(28) Heyne, S.; Roubaud, A.; Ribaucour, M.; Vanhove, G.; Minetti, R.; Favrat, D. *Fuel* **2008**, *87*, 3046.
(29) Gersen, S.; Anikin, N. B.; Mokhov, A. V.; Levinsky, H. B. *Int. J. Hydrogen Energy* **2008**, *33*, 1957.
(30) Cheng, R. K.; Oppenheim, A. K. *Combust. Flame* **1984**, *58*, 125.
(31) Petersen, E. L.; Kalitan, D. M.; Simmons, S.; Bourque, G.; Curran, H. J.; Simmie, J. M. *Proc. Combust. Inst.* **2007**, *31*, 447.
(32) Healy, D.; Curran, H. J.; Dooley, S.; Simmie, J. M.; Kalitan, D. M.; Petersen, E. L.; Bourque, G. *Combust. Flame* **2008**, *155*, 451.
(33) Healy, D.; Curran, H. J.; Simmie, J. M.; Kalitan, D. M.; Zinner, C. M.; Barrett, A. B.; Petersen, E. L.; Bourque, G. *Combust. Flame* **2008**, *155*, 441.
(34) Bourque, G.; Healy, D.; Curran, H.; Zinner, C.; Kalitan, D.; de Vries, J.; Aul, C.; Petersen, E. *Proc. ASME Turbo Expo.* **2008**, *3*, 1051.

Table 2. Summary of Ignition Delay Data Available for Hydrocarbon Blends

author	blends	T/K	P/bar	ϕ
Higgin and Williams[9]	CH_4/C4	1800−2500	0.2−0.4	0.5
Crossley et al.[35]	CH_4/C_2-C_5	1400−2000	0.2	1.0
Eubank et al.[36]	CH_4/C_2-C_4	1200−1850	4.0	0.2−0.4
Zellner et al.[37]	CH_4/C_2-C_4	1400−2000	3.0	0.2
Krishnan et al.[38]	CH_4/C_2H_2	1700−1900	1−4	0.5−2.0
Spadaccini and Colket[1]	CH_4/C_2-C_4	1300−2000	3−15	0.45−1.25
Cheng and Oppenheim[30]	CH_4/H_2	800−2400	1−3	0.5−1.25
Frenklach and Bornside[39]	CH_4/C_3	1300−1600	2.5	1.0
Goy et al.[40]	CH_4/C_2-C_3	900−1600	5−40	0.5−1.0
Lamoureux and Paillard[41]	CH_4/C_2-C_3	1485−1900	3−13	0.5−2.0
Kim et al.[24]	C_3H_8/n-C_4H_{10}	720−900	16−18	1.0
El Bakali et al.[42]	CH_4/C_2-C_6	1300−1800	0.1	0.75−1.5
Huang and Bushe[43]	CH_4/C_2-C_3	900−1400	16−40	1.0
Petersen et al.[44]	CH_4/C_2-C_3, H_2	1200−2000	1.0−25	0.5
Healy et al.[32,33]	CH_4/C_3H_8	740−1550	10−30	0.3−3.0
	$CH_4/C_2H_6/C_3H_8$	770−1580	1−50	0.5−2.0
Heyne et al.[28]	CH_4/C_2-C_3	850−925	13−21	0.6−1.0
Gersen et al.[29]	CH_4/H_2	950−1060	15−70	0.5−1.0
Bourque et al.[34]	C_1-C_5	740−1660	1−33	0.3−2.0
de Vries et al.[45]	CH_4/C_2-C_5	750−1600	1−30	0.5−2.0
Herzler et al.[46]	CH_4/C_3, H_2	900−1800	1−16	0.5−1.0

temperatures from 740 to 1660 K. Laminar flame speeds were also measured at pressures up to 4 bar using a high-pressure vessel with optical access. Two different fuel blends containing ethane, propane, *n*-butane, and *n*-pentane added to methane were studied in the shock tubes (only one blend was studied in the RCM) at equivalence ratios varying from lean (0.3) to rich (2.0). This work presented the most comprehensive set of experimental ignition and laminar flame speed data available in the open literature for $CH_4/C_2H_6/C_3H_8/C_4H_{10}/C_5H_{12}$ fuel blends with significant levels of C2+ hydrocarbons. With the use of these data, a detailed chemical kinetics model was compiled and refined. The predictions of the model were very good over the entire range of ignition delay times.

2. Specific Objectives

This current body of work is designed to build upon and complement our previous investigations into the oxidation of comparable natural gas blends of CH_4/C_3H_8,[32] $CH_4/C_2H_6/C_3H_8$,[33] and $CH_4/C_2H_6/C_3H_8/n$-C_4H_{10}/n-C_5H_{12}[34] in our laboratories. Herein, we extend the envelope of the aforementioned quinternary mixture from one containing approximately 80% methane with reducing concentrations of progressively larger higher order hydrocarbons to one composing approximately 62% methane and thus has relatively higher concentrations of larger hydrocarbon species. Most specifically, the rapid compression machine data presented in this current study for the 62% methane mixture (NG3) has not been previously presented. Our intention is to make the study applicable to nontraditional sources of fuels such as coal-derived natural gas blends which may contain higher than normal concentrations of components that are more reactive compared to methane. The work reports ignition delay measurements at three equivalence ratios and three pressures following a range of conditions similar to those studied in our previous investigations.

These experimental data have been used to validate a detailed chemical kinetic model containing a comprehensive representation of low-temperature chemistry for fuels up to and including *n*-pentane. Overall, the model accurately reproduces the observed experimental dependencies on temperature, pressure, equivalence ratio, and mixture composition.

3. Experiment and Model

Experiments were conducted in two high-pressure shock tubes and in a rapid compression machine. The first shock tube has a 10.7 m driven section with an inner diameter of 16.2 cm and a 3.5 m driver section. The second shock-tube facility has a 4.72 m test section with an internal diameter of 15.24 cm and a 2.46 m driver section with an internal diameter of 7.62 cm. Both shock tubes were fitted with counters (Fluke PM 6666) linked to a series of pressure transducers (PCB 113) near the endwall. The presence of chemical reactivity in the reflected-shock region is detected by pressure transducers (PCB 134A and 603B1) and photomultiplier tubes (Hamamatsu 1P21) located at the endwall and on the sidewall 1.6 cm from the endwall. Further details on the shock-tube experiments and results utilized herein are provided in Bourque et al.[34]

The twin piston rapid compression machine (RCM) used[47] has an effective compression ratio of approximately 10:1 and a compression time of approximately 16 ms. The stainless steel combustion chamber can be charged with an initial pressure of up to 2 bar, has a maximum working tolerance of 200 bar, and has an operating temperature in the region of 600−1100 K, conditions analogous to those found in gas turbines. Creviced pistons are utilized to reduce mixing of boundary and core gases during the compression stroke leading to greater homogeneity of temperature after compression.[48] A Horst heating tape was used to vary the initial temperature of the chamber between 290 and 380 K. Pressure dynamics in the combustion chamber were measured by

(35) Crossley, R. W.; Dorko, E. A.; Scheller, K.; Burcat, A. *Combust. Flame* **1972**, *19*, 373.
(36) Eubank, C. S.; Rabinowitz, M. J.; Gardiner, W. C., Jr.; Zellner, R. E. *Proc. Combust. Inst.* **1981**, *18*, 1767.
(37) Zellner, R.; Niemitz, K. J.; Warnatz, J.; Gardiner, W. C., Jr.; Eubank, C. S.; Simmie, J. M. *Prog. Aeronaut. Astronaut.* **1983**, *80*, 252.
(38) Krishnan, K. S.; Ravikumar, R.; Bhaskaran, K. A. *Combust. Flame* **1983**, *49*, 41.
(39) Frenklach, M.; Bornside, D. E. *Combust. Flame* **1984**, *56*, 1.
(40) Goy, C. J.; Moran, A. J.; Thomas, G. O. *ASME*, 2001; Paper 2001-GT-0051.
(41) Lamoureux, N.; Paillard, C.-E. *Shock Waves* **2003**, *13*, 57.
(42) El Bakali, A.; Dagaut, P.; Pillier, L.; Desgroux, P.; Pauwels, J.-F.; Rida, A.; Meunier, P. *Combust. Flame* **2004**, *137*, 109.
(43) Huang, J.; Bushe, W. K. *Combust. Flame* **2006**, *144*, 74.
(44) Petersen, E. L.; Hall, J. M.; Smith, S. D.; de Vries, J.; Amadio, A.; Crofton, M. *J. Eng. Gas Turbines Power* **2007**, *129*, 937.
(45) de Vries, J.; Petersen, E. L. *Proc. Combust. Inst.* **2009**, *21*, 3163.
(46) Herzler, J.; Naumann, C. *Proc. Combust. Inst.* **2009**, *32*, 213.
(47) Affleck, W. S.; Thomas, A. *Proc. Inst. Mech. Eng.* **1968**, *183*, 365.
(48) Würmel, J.; Simmie, J. M. *Combust. Flame* **2003**, *141*, 417.

Table 3. Fractional Composition of Fuel Blends

species	NG2	NG3
CH_4	0.8128	0.6250
C_2H_6	0.1000	0.2000
C_3H_8	0.0500	0.1000
n-C_4H_{10}	0.0250	0.0500
n-C_5H_{12}	0.0125	0.0250

a Kistler 603B pressure transducer in combination with a Kistler 5007 amplifier. The pressure/time profiles were recorded on a Nicolet Sigma 90-4 oscilloscope at a resolution of 1 megasamples/s. Chamber windows were replaced with aluminum blanks to reinforce its integrity; this was necessary as the maximum tolerance of the chamber was breached on several occasions upon ignition. Ignition delay time (τ) was defined as the time from the peak pressure as a result of the rapid compression to the rapid rise in pressure due to the onset of ignition. Fuels used were CH_4 (>99.99% purity), C_2H_6 (>99.99%), C_3H_8 (>99.97%), n-C_4H_{10} (>99.97%), and n-C_5H_{12} (>99.97%). These fuels were premixed in a separate tank before mixing with oxygen and diluent in the final mixture preparation. This approach was adopted in order to reduce error in preparing what finally becomes a seven-component mixture. The partial pressure of each gaseous component was measured using a regularly calibrated Edwards ASG 2000 mbar pressure gauge. Fuel reservoirs were first evacuated and then "washed" with the bath gases they were to contain before final mixture preparation. The gaseous mixtures were then allowed to homogenize by the processes of stirring and convection for a minimum of 8 h before transfer to the combustion chamber.

Table 3 shows the gas compositions studied in the temperature range 630−1540 K. It must be noted that for shock-tube experiments N_2 is the only diluent used, whereas for the RCM experiments both 100% N_2 and 100% Ar bath gases were necessary to investigate the entire temperature envelope. Varying the initial temperature of the combustion chamber also gave more flexibility and control over the compressed gas temperatures explored. It must also be noted that the compositions of the test gases are not typical for natural gas; they are extreme and have been specifically designed to broaden the test parameters of the model.

The chemical kinetic mechanism was developed and simulations performed using the HCT (hydrodynamics, chemistry, and transport) program.[49] The detailed chemical kinetic model is based on the hierarchical nature of hydrocarbon combustion mechanisms containing the H_2/O_2 submechanism,[50] together with the CO/CH_4 and larger hydrocarbon submechanisms. The C4 and C5 submechanism are based on the rate reaction rules of Curran et al.[51,52] The version of the model used in this work is C5_49 and consists of 293 species and 1588 reactions. A complete listing of the detailed kinetic mechanism is available online at http://c3.nuigalway.ie/mechanisms.html together with associated thermochemical parameters.

4. Results and Discussion

Ignition delay times measured in RCMs can range from 3 to 250 ms, thus allowing a significant time for heat losses to affect and complicate ignition delay time measurements. RCM experimental data are provided as Tables 1−17 in the Supporting Information, while shock-tube results constitute Tables 18−33. Note that for the shock-tube results the measured pressure is usually higher at lower temperature and relatively lower at higher temperature for each mixture composition studied, as the reflected shock pressure is individual to each experiment and is a function of the shock velocity, initial pressure, and temperature and the nature of the individual shock wave.

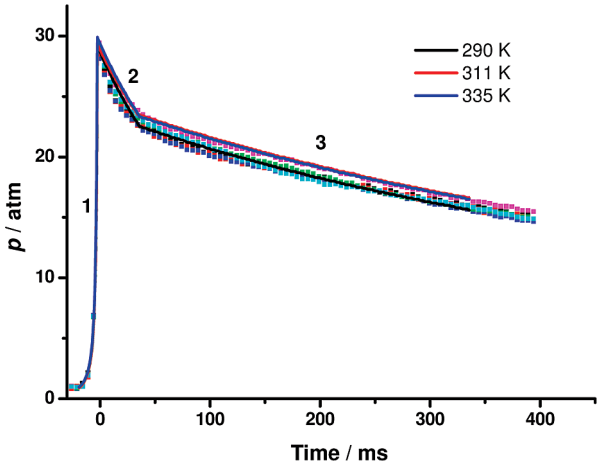

Figure 1. Simulation of measured pressure profile of a nonreactive NG3 mixture at $\phi = 0.5$, $p = 30$ bar with 100% Ar as diluent.

In order to account for heat losses in the rapid compression machine, a number of nonreactive experiments were performed in which the O_2 content of the mixture was replaced with N_2 and then simulated. This type of simulation has been described by us previously[17] but is discussed briefly here again. Figure 1 shows the comparison of simulation and measurement of a nonreactive pressure trace. In this figure, three different initial temperatures are simulated at 290, 311, and 335 K.

There are three distinct regions in the trace. The first is the compression phase, the second immediately after compression in which the greatest pressure drop (and associated heat loss) occurs and the third region in which there is a lesser but still considerable heat loss. These regions are common to all of the RCM experiments performed, and they have already been reported in our other natural gas studies.[17,32,33] We are not certain what actually causes the different cooling in regions 2 and 3, it may be due to some slight expansion after compression in region 2 followed by a more consistent heat conduction in region 3. We simulate each compression using the initial experimental temperature and pressure and the compression ratio calculated using these and the measured compressed gas pressure from the isentropic relationship:

$$\ln\left(\frac{p_c}{p_i}\right) = \int_{T_i}^{T_C} \frac{\gamma}{\gamma - 1}\frac{dT}{T}$$

Heat losses for regions 2 and 3 are derived by simulating pressure traces of nonreactive mixtures (mixtures in which O_2 was replaced by N_2) by treating each as an adiabatic expansion, with region 2 expanding at a faster rate compared with region 3, so that the simulated pressure profile reproduces that which was measured experimentally. The parameters, such as compression ratio and rate of expansion, so derived were then applied to the simulation of the reactive experiments. Heat losses were simulated for the full range of temperature, pressure, equivalence ratio, and diluent composition investigated in the reactive study. This type of simulation was

(49) Lund, C. M.; Chase, L. *HCT-A General Computer Program for Calculating Time-Dependent Phenomena Involving One-Dimensional Hydrodynamics, Transport, and Detailed Chemical Kinetics*, Lawrence Livermore National Laboratory Report UCRL-52504, revised 1995.
(50) O Conaire, M.; Curran, H. J.; Simmie, J. M.; Pitz, W. J.; Westbrook, C. K. *Int. J. Chem. Kinet.* **2004**, *36*, 603.
(51) Curran, H. J.; Gaffuri, P.; Pitz, W. J.; Westbrook, C. K. *Combust. Flame* **1998**, *114*, 149.
(52) Curran, H. J.; Gaffuri, P.; Pitz, W. J.; Westbrook, C. K. *Combust. Flame* **2002**, *129*, 253.

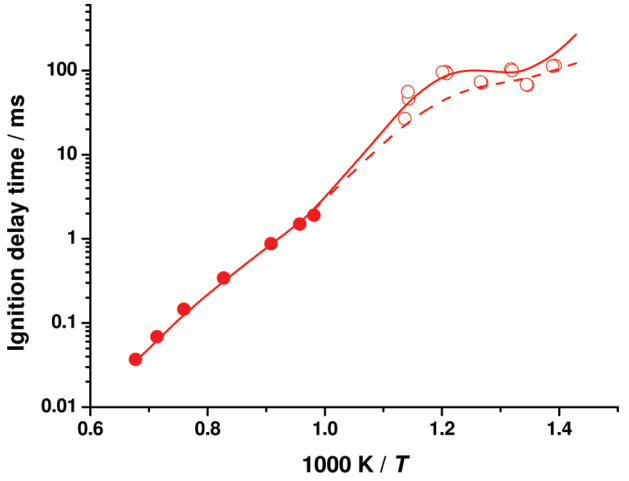

Figure 2. NG 3 oxidation, $\phi = 2.0$ in air, 20 bar; red ●, ST; red ○, RCM; solid line, heat loss; dashed line, adiabatic simulation.

proposed and used by Mittal et al.[53] in simulating their H_2/CO RCM experiments. We have also applied this same methodology to our recent work on propane oxidation in an RCM with reasonable success,[17] in that the model was reasonably accurate in reproducing the experimental results, but there was still some disagreement between the experiment and model. Comparisons of experimental results and model simulations of unreactive mixtures are provided in the Supporting Information. In all the model calculations and comparisons to experiment which follow, the calculated curve contains within it the effects of heat loss and the corresponding decrease in pressure over time, of which Figure 1 is an example.

Of course, the heat losses in the real RCM create a nonuniform temperature gradient as a result of the colder layer of gases adjacent to the walls. While a true multidimensional simulation would be able to capture such a nonuniform temperature field, performing such calculations in conjunction with the full chemistry model is impractical and virtually impossible given the current state of the art of computational fluid mechanics solvers. The authors feel that modeling the temperature loss in terms of a bulk, zero-dimensional pressure and temperature that changes with time, as described above, sufficiently captures the heat loss effects and does so in a way that can be coupled with the full chemical kinetics.

Heat losses were not considered for the shock-tube experiments as the time scale in these experiments is much shorter than those in a RCM. The dashed line in Figure 2 represents the simulation of the RCM experiments assuming adiabatic conditions. While the simulation accurately predicts the reactivity of the high-temperature shock-tube experiments, it overpredicts the reactivity of the system for the lower-temperature RCM experiments. When heat losses are considered in the simulation of RCM experiments, not only is the simulation more realistic but also the negative temperature dependence becomes more pronounced and is more accurately portrayed in the temperature range 740−820 K. In all the model calculations and comparisons to experiment which follow, the calculated curve contains within it the effects of heat loss and the corresponding decrease in pressure over time, of which Figure 1 is an example. As indicated in Figure 2, the shock-tube and RCM data and calculated curves are labeled as being at 20 atm; this nomenclature is for convenience, and for the shock-tube data it represents the average pressure prior to ignition, and for the RCM data is represents the peak pressure. Even though the model curve is labeled as 20 atm, the true RCM pressure history, as described above, was employed in each calculation. Similar nomenclature and methods are used throughout the rest of this article when showing the data and model results. Also, for all figures, the solid lines represent the model predictions.

4.1. Effect of Pressure. Natural gas mixtures were studied at pressures of 10, 20, and 30 bar, at fuel/"air" equivalence ratios (ϕ) of 0.5, Figure 3, $\phi = 1.0$, Figure 4, and $\phi = 2.0$, Figure 5, for NG2 (a) and NG3 (b). Figure 3a shows that the ignition limits recorded experimentally at both 10 and 20 bar are correctly predicted by the model, and it also captures the overall reactivity at 10 bar but overpredicts reactivity at 20 bar and at $\phi = 0.5$. At 30 bar and at all equivalence ratios, the model accurately captures fuel reactivity at temperatures above 900 K and predicts the negative temperature coefficient (NTC) behavior of the fuel quite well. However, it consistently under-predicts the reactivity at lower temperatures.

For the NG3 blend, Figures 3, 4, and 5b, the ignition limits at 20 and 30 bar occur at approximately 735 K but the ignition limit at 10 bar occurs around 990 K. The onset of reactivity for both 20 and 30 bar occurs at the beginning of a region of negative temperature dependence, 740−850 K. This NTC region is present at all equivalence ratios for 30 bar, but at 20 bar it is only observed at stoichiometric and rich conditions. The ignition limit for 10 bar experiments occurs at a temperature above the NTC region so only a positive temperature dependence is observed at this pressure.

Although the model is slower than experiments at low temperatures and higher pressures, it does reproduce the general trends of the experimental data quite well; the NTC region is accurately captured, and the ignition limits at all three pressures are very well reproduced. Finally, as we noted earlier, Tables 18−33 of the Supporting Information show that the shock-tube experimental data are not recorded at the constant reflected shock pressure, with normally higher reflected shock pressures at lower temperatures and lower pressures at higher temperatures. In simulating this data, we use the measured experimental pressure at each temperature to accurately simulate the experimental data. However, this results in a reduced apparent pressure dependence at higher temperatures.

4.2. Effect of Equivalence Ratio. Contrasts are also available for reactivity at varying equivalence ratios (0.5, 1.0, and 2.0) at 10 bar pressure, Figure 6, at 20 bar, Figure 7, and at 30 bar, Figure 8. For both NG2 and NG3 mixtures at 10 bar, Figure 6, we observe a "turnover" in reactivity at about 1250 K. At temperatures below this turnover, fuel-rich mixtures are *fastest* and fuel-lean *slowest* to ignite; however, at temperatures above 1250 K, the opposite is true, with fuel-rich mixtures *slowest* to ignite with fuel-lean mixtures being *fastest*. This difference in behavior is due to the different chemistry responsible for fuel oxidation in the different temperature regimes. At lower temperatures, 600−900 K, reactivity depends on the low-temperature fuel oxidation mechanism, in which fuel alkyl radicals add to molecular oxygen, with subsequent internal hydrogen atom rearrangements leading to chain-branching. At intermediate temperatures, 900−1250 K, reactivity depends on hydroperoxyl radical chemistry, namely, $RH + H\dot{O}_2 = \dot{R} + H_2O_2$ with

(53) Mittal, G.; Sung, C. J.; Fairweather, M.; Tomlin, A. S.; Griffiths, J. F.; Hughes, K. J. *Proc. Combust. Inst.* **2007**, *31*, 419.

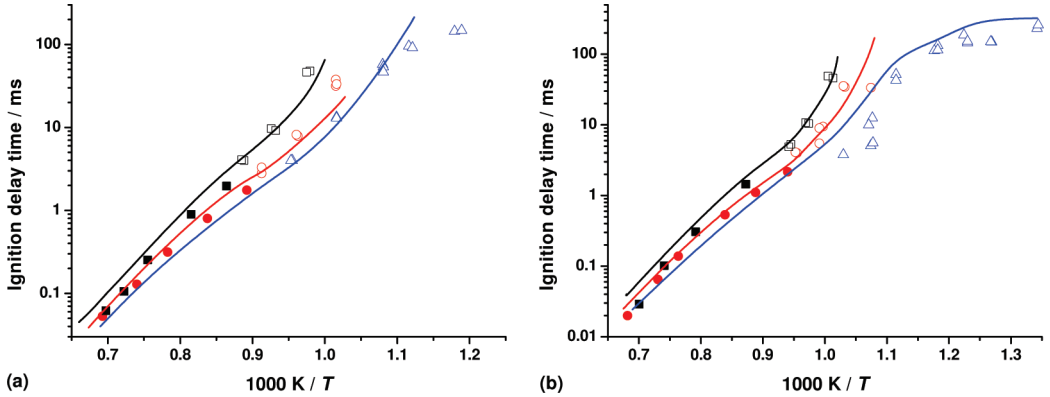

Figure 3. Effect of pressure on NG2 (a) and NG3 (b) ignition, $\phi = 0.5$, in "air"; □, RCM 10 bar; ■, shock tube 8 bar; red ○, RCM 20 bar; red●, shock tube 19 bar; blue △, RCM 30 bar. Solid lines, simulation including heat loss.

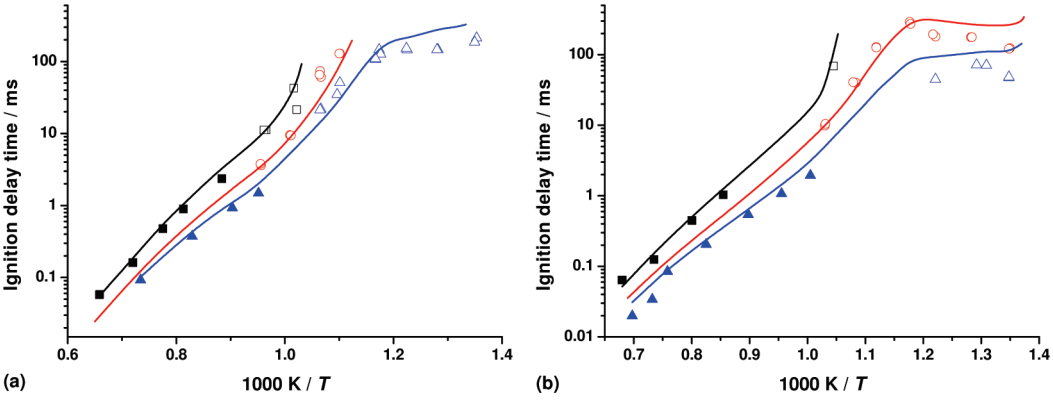

Figure 4. Effect of pressure on NG2 (a) and NG3 (b) ignition, $\phi = 1.0$, in "air"; □, RCM 10 bar; ■, shock tube 8 bar; red ○, RCM 20 bar, blue △, RCM30 bar; blue ▲, shock tube 30 bar. Solid lines, simulation including heat loss.

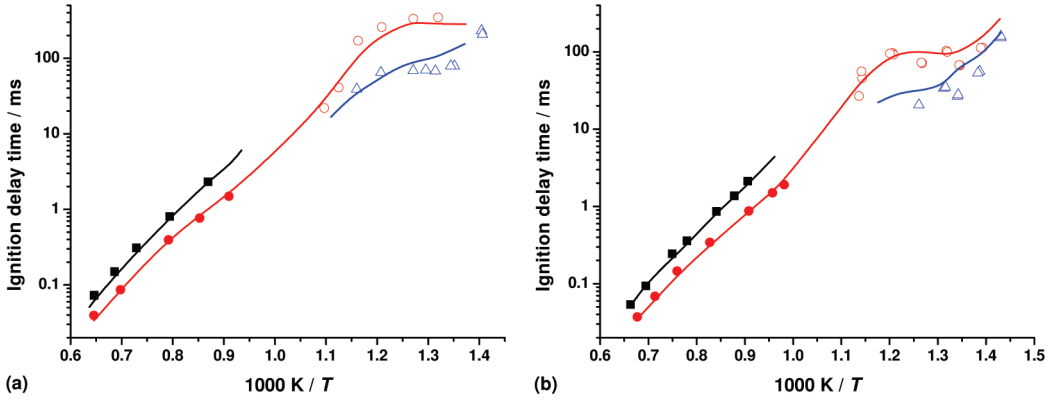

Figure 5. Effect of pressure on NG2 (a) and NG3 (b) ignition, $\phi = 2.0$, in "air"; ■, shock tube 8 bar; red ○, RCM 20 bar; red ●, shock tube 18 bar; blue △, RCM 30 bar. Solid lines, simulation including heat loss.

the subsequent decomposition of hydrogen peroxide into two hydroxyl radicals, leading to chain-branching. Finally, at temperatures above 1250 K, chain branching stems from the reaction $\dot{H} + O_2 = \ddot{O} + \dot{O}H$, and the rate of this reaction is limited by the concentration of molecular oxygen. Thus, fuel-lean mixtures are most reactive at high temperatures.

The model shows the same trends as the experiment; the order of reactivity is captured correctly, ignition limits of the fuel are accurately reproduced, and the overall behavior of the fuel is well represented by the model, particularly the transition from low- to intermediate- and to high-temperature kinetics. It reproduces the entire ignition profile for all equivalence ratios and at all pressures for both natural gas blends.

It is interesting to note that the temperature at which the "turnover" from low- to high-temperature kinetics moves to higher temperature with increasing pressure. As reported above, this transition occurs at a temperature of approximately 1250 K at 10 bar, Figure 6, but shifts to approximately 1400 K at 20 bar, Figure 7. This feature is also reproduced by the model. However, experiments at 30 bar were not performed at temperatures high enough to see the "turnover" temperature.

We have presented what we believe to be a convincing argument to explain the reactivity of the blends showing a

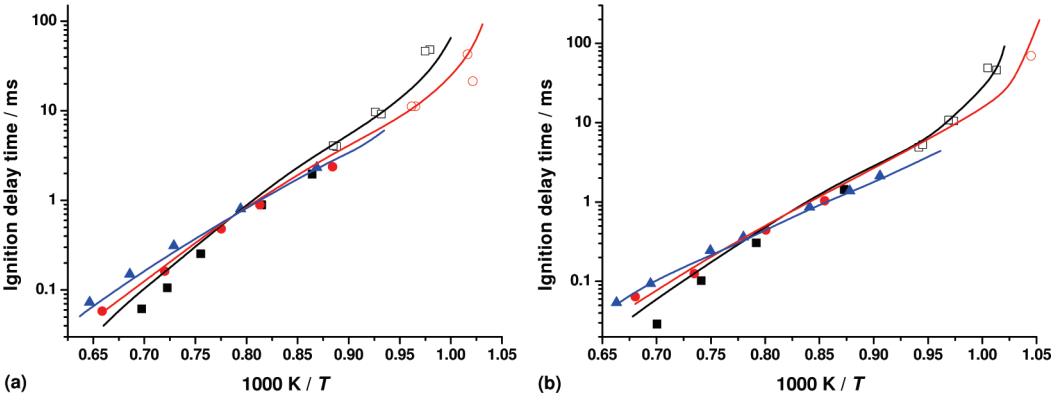

Figure 6. Effect of equivalence ratio on NG2 (a) and NG3 (b) ignition in air, $p = 10$ bar; □, RCM $\phi = 0.5$; ■, shock tube $\phi = 0.5$; red ○, RCM $\phi = 1.0$; red ●, shock tube $\phi = 1.0$; blue ▲, shock tube $\phi = 2.0$. Solid lines, simulation including heat loss.

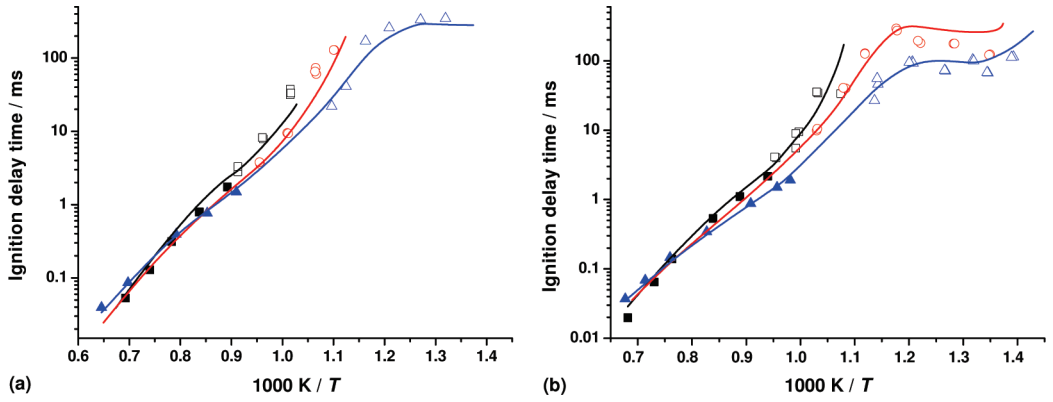

Figure 7. Effect of equivalence ratio on NG2 (a) and NG3 (b) ignition in air, $p = 20$ bar, □ − RCM $\phi = 0.5$, ■ − shock tube $\phi = 0.5$, red ○, RCM $\phi = 1.0$; blue △, RCM $\phi = 2.0$; blue ▲, shock tube $\phi = 2.0$. Solid lines, simulation including heat loss.

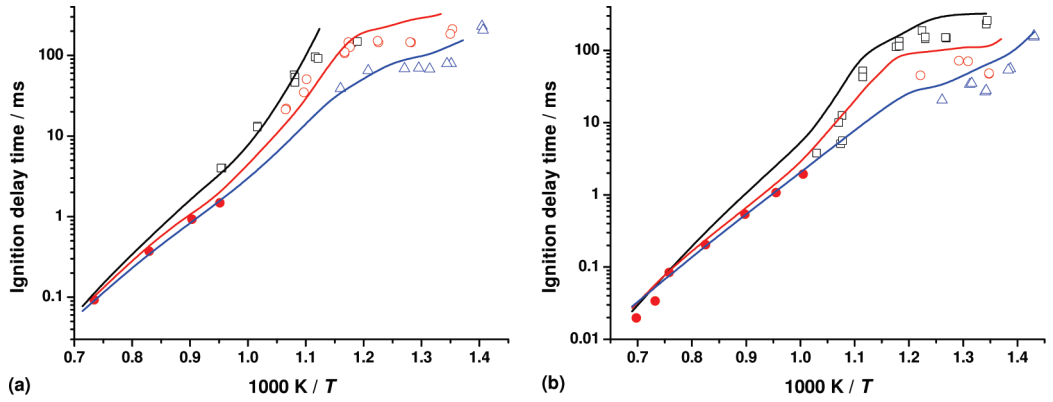

Figure 8. Effect of equivalence ratio on NG2 (a) and NG3 (b) ignition in air, $p = 30$ bar, □, RCM $\phi = 0.5$; red ○, RCM $\phi = 1.0$; blue △, RCM $\phi = 2.0$. Solid lines, simulation including heat loss.

"turnover" of the reactivity going from high to low temperature, which different stoichiometries are considered. This turnover is seen at 10 bar, Figure 6, but appears slightly "washed out" at higher pressures, Figures 7 and 8, due to the fact that the measured reflected shock pressure decreases at higher temperatures while the simulation uses the experimental values, see Tables 18−33 of the Supporting Information.

4.3. Effect of Natural Gas Composition. The reactivities of NG2 and NG3 mixtures are compared in Figure 9. NG3 is the more reactive of these two fuel blends as expected because it contains a greater fraction of higher order hydrocarbons. At $\phi = 1.0$ and 10 bar, Figure 9a, the experiments indicate that there is a significant decrease in activation energy at temperature increases from approximately 950 to 1000 K. The model accurately captures the two different regions of reactivity for both NG mixtures. The temperature at which the transition between these two regions occurs (1000 K) is also the temperature of transition of the accessible experimental temperature envelope from the RCM to the shock-tube experiments.

At high temperatures, the experimental ignition profile at $\phi = 1.0$ and 30 bar, Figure 9b, is accurately reproduced by the model, and the high-temperature end of the NTC region is also captured very well. The model predicts the overall behavior of both blends with reasonable accuracy but is

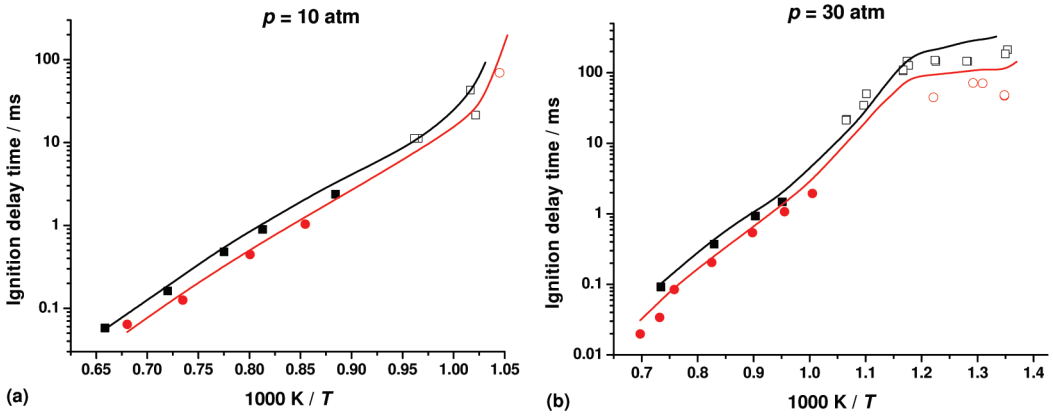

Figure 9. Effect of natural gas composition on ignition at $\phi = 1.0$ in "air", (a) $p = 10$ bar and (b) $p = 30$ bar; □, RCM NG2; ■, shock tube NG2; red ○, RCM NG3; red ●, shock tube NG3. Solid lines, simulation including heat loss.

slightly slower compared with experiments at lower temperature and higher pressure.

Even though there are considerable heat losses associated with the RCM experiments at long ignition times and little or no heat losses in the shock tube, there is very good agreement between both sets of data where overlap occurs. For the highest-temperature experiments in the RCM, ignition delay times are short, typically in the range 35 ms, and heat losses are minimal. Thus, where conditions overlap, it is encouraging to observe this agreement between shock-tube and RCM measurements. Also included are comparisons of both natural gas mixtures at $\phi = 0.5$ and $\phi = 2.0$, as Figures 1 and 2 of the Supporting Information, which highlight the fact that NG3 is more reactive at all conditions compared to NG2.

5. Conclusions

Overall there is very good agreement between the model and experiment for the conditions reported. There is however an improvement to be made in the model to account for the poorer agreement at high pressure and low temperature. Because the model can already reliably reproduce most of the data, the ignition behavior of the fuels such as ignition limits and negative temperature dependence means that the current version of the model lays a solid foundation for future development. This work contributes a large body of data to the combustion community that will be useful in the development and improvement of models to simulate natural gas oxidation or the oxidation of similar fuels derived from other sources at a variety of conditions.

Acknowledgment. Financial support is much appreciated from Rolls-Royce Canada Ltd. and The Higher Education Authority of Ireland. Additional support came from the U.S. National Science Foundation, Grant Number CBET-0832561.

Supporting Information Available: A full listing of the RCM data, Tables 1−17, shock tube data, Tables 18−33, in addition to experimental pressure profiles recorded for a series of unreactive mixtures and the parameters which were used to develop a heat loss model. This material is available free of charge via the Internet at http://pubs.acs.org.